Environmental Effects of Waveguide Uncertainty on Coherent Aspects of Propagation, Scattering and Reverberation

Kevin D. LePage and B. Edward McDonald

Naval Research Laboratory, 4555 Overlook Ave. SW, Washington, DC 20375

Abstract. The robustness of the coherence of waveguide propagation to environmental uncertainty becomes an important consideration for systems that seek to exploit coherence for gain. Examples include matched field processing for passive localization and Time Reversal Mirrors (TRMs) for active systems. Here efficient normal mode representations of mid-frequency time domain propagation using the narrowband and adiabatic approximations are used to explore the deterioration of active system predictability and performance in the presence of environmental fluctuations (i.e. sound speed perturbations in the water column and/or bottom, or bathymetry fluctuations). Results show that for TRMs the reverberation level at the focal range is increased, and the scattering from an illuminated object is reduced for ensembles over environmental uncertainty. Results are obtained analytically as formal averages and are believed to represent a lower limit on the deterioration of TRM performance in the presence of environmental uncertainty for actual waveguides.

INTRODUCTION

Uncertainty in waveguide properties causes commensurate uncertainty in acoustic propagation, scattering and reverberation in shallow water waveguides. In cases where knowledge of the spatial scales of waveguide variability and the associated variances are known, it is possible to quantify the uncertainty of the acoustic quantities of interest under the statistical hypothesis of homogeneity to various levels of fidelity (travel time perturbations to rays or modes, vs. full wave modeling). Representations based on the assumption that environmental perturbations cause only phase and travel-time perturbations offer value for estimating the lower bound of acoustic uncertainty. Here the adiabatic approach developed by Krolik [1] for modeling the predictability of the co-intensity of coherent propagation of normal modes through internal wave fields at a single frequency is extended to the time domain, and consistent expressions are obtained for modeling the predictability of boundary reverberation and target scattering. Such expressions are believed to represent a lower bound for the propagation of environmental uncertainty into acoustic uncertainty.

THEORY

The adiabatic theory for time domain propagation in normal modes has been derived previously [2,3]. However, for the sake of completeness, we briefly review. Complex envelope theory may be used to integrate adiabatic mode solutions to the Helmholtz equation [4] over a Gaussian weighted frequency to obtain

$$p\left(t,r,z_s,z\middle|\omega,\Delta\omega\right)=\frac{2}{\rho\left(z_s\right)\sqrt{r}}\mathrm{Re}\left\{e^{-i(\omega t+\pi/4)}\sum_{n=1}^{N}\frac{\exp\left(i\left\langle k_n\right\rangle_r r-\dfrac{\left(t-\left\langle S_n\right\rangle_r r\right)^2/2}{\left(\Delta\omega^{-2}-i\left\langle D_n\right\rangle_r r\right)}\right)}{\sqrt{\left\langle k_n\right\rangle_r\left(\Delta\omega^{-2}-i\left\langle D_n\right\rangle_r r\right)}}\phi_n\left(z_s,0\right)\phi_n\left(z,r\right)\right\}, \tag{1}$$

where $\Delta\omega$ is the bandwidth, $\langle\ \rangle_r$ indicates range average and S_n and D_n are the first and second derivatives w.r.t. frequency of the wavenumber k_n. It is assumed that k_n and S_n deviate from their mean value by their first perturbations w.r.t. the environmental sound speed defect $\Delta c\left(r,z\right)$ [5]

$$k_n=k_n^0-\frac{\omega}{k_n^0}\int_{-\infty}^{0}\frac{\Delta c\left(r,z\right)}{c^3\left(z\right)\rho\left(z\right)}\phi_n^2\left(z\right)dz, \tag{2}$$

and

$$S_n=S_n^0-\left(2-S_n\frac{\omega}{k_n^0}\right)\frac{\omega}{k_n^0}\int_{-\infty}^{0}\frac{\Delta c\left(r,z\right)}{c^3\left(z\right)\rho\left(z\right)}\phi_n^2\left(z\right)dz-2\frac{\omega^2}{k_n^0}\int_{-\infty}^{0}\frac{\Delta c\left(r,z\right)}{c^3\left(z\right)\rho\left(z\right)}\frac{\partial\phi_n\left(z\right)}{\partial\omega}\phi_n\left(z\right)dz. \tag{3}$$

It is also assumed that the modal dispersions D_n are independent of the environmental variability for reasons of analytic tractability.

An EOF decomposition of the sound speed perturbations is adopted [1]

$$\Delta c\left(r,z\right)=\sum_{e=1}^{E}g_e\left(r\right)\psi_e\left(z\right). \tag{4}$$

Equation (4) assumes that the perturbations are separable into orthogonal depth functions ψ_e and uncorrelated random amplitudes g_e. These latter are distributed Gaussian in amplitude and are characterized spatially by a Gaussian correlation function with length scale l_e. Under this model the range integrated wavenumbers and slownesses are

$$\left\langle k_n\right\rangle_r r=k_n^0 r-\frac{\omega}{k_n^0}\sum_{e=1}^{E}N\left(0,\sigma_{g_e}^2 r l_e\right)\int_{-\infty}^{0}\frac{\psi_e\left(z\right)}{c^3\left(z\right)\rho\left(z\right)}\phi_n^2\left(z\right)dz, \tag{5}$$

and

$$\left\langle S_n\right\rangle_r r=S_n^0 r-\frac{\omega}{k_n^0}\sum_{e=1}^{E}N\left(0,\sigma_{g_e}^2 r l_e\right)\left(\left(2-\frac{\omega}{k_n^0}\right)\int_{-\infty}^{0}\frac{\psi_e\left(z\right)}{c^3\left(z\right)\rho\left(z\right)}\phi_n^2\left(z\right)dz+\omega\int_{-\infty}^{0}\frac{\psi_e\left(z\right)}{c^3\left(z\right)\rho\left(z\right)}\frac{\partial\phi_n}{\partial\omega}\phi_n\left(z\right)dz\right) \tag{6}$$

where $N\left(0,\sigma^2\right)$ is a zero mean Gaussian random variable with variance σ^2.

Propagation Uncertainty

Equations (5) and (6) indicate that the uncertainties in the total accumulated phase and travel time have variances proportional to the horizontal correlation length scale of the environmental sound speed defects multiplied by the range. The short-time average of the acoustic co-intensity from a TRM may be written as [2]

$$
\begin{aligned}
\left\langle p_{TRM}(t_1,r,z_1)\, p_{TRM}(t_2,r,z_2)\right\rangle &= 2\mathrm{Re}\Bigg\{ \frac{4p^2}{\Delta z^2 r^2(z_p)\, rR_p} \sum_{n=1}^{N}\sum_{m=1}^{M} \frac{e^{i\left(k_n-k_m^*\right)r - i\left(k_n^*-k_m\right)R_p}}{|k_n||k_m|} f_n(z_p)\, f_m(z_p)\, f_n(z) f_m(z) \\
&\times \quad \frac{1}{4p^2}\int_{-\infty}^{\infty} dw_1 \int_{-\infty}^{\infty} dw_2\, e^{-iw_1\left(t_1 - S_n r + S_n R_p\right)} e^{iw_2\left(t_2 - S_m r + S_m R_p\right)} \\
&\times \quad \prod_{e=1}^{E} e^{-\left(\Delta k_{en}-\Delta k_{em}+w_1\Delta S_{en}-w_2\Delta S_{em}\right)^2 r l_e s_{g_e}^2/2} \Bigg\}
\end{aligned}
\quad , (7)
$$

where

$$
\Delta k_{en} = -\frac{w}{k_n^o}\int_{-\infty}^{o} \frac{j_e(z)}{c^3(z)\, r(z)} f_n^2(z)\, dz, \tag{8}
$$

and

$$
\Delta S_{en} = -\left(2-\frac{w}{k_n^o}\right)\frac{w}{k_n^o}\int_{-\infty}^{o} \frac{j_e(z)}{c^3(z)\, r(z)} f_n^2(z)\, dz - \frac{w^2}{k_n^o}\int_{-\infty}^{o} \frac{j_e(z)}{c^3(z)\, r(z)} \frac{\partial f_n}{\partial w} f_n(z)\, dz. \tag{9}
$$

Equation (7) may be integrated w.r.t. w_1 and w_2 giving

$$
\begin{aligned}
&\left\langle p_{TRM}(t_1,\Delta r+R_p,z_1)\, p_{TRM}(t_2,\Delta r+R_p,z_2)\right\rangle = \frac{2p}{\Delta z^2 r^2(z_p)\, rR_p} \sum_{n=1}^{N}\sum_{m=1}^{M} \frac{e^{i\left(\mathrm{Re}(k_n-k_m)\Delta r - \mathrm{Im}(k_n+k_m)(\Delta r+2R_p)\right)}}{|k_n||k_m|} f_n(z_p)\, f_m(z_p)\, f_n(z)\, f_m(z) \\
&\times \exp\left(-\Theta_{nm}^2\right)\left(\Theta_{22}^2+\left(\Delta w^{-2}+iD_m\Delta r\right)/2\right)^{-1/2} \left(\Theta_{11}^2+\left(\Delta w^{-2}-iD_n\Delta r\right)/2 - \frac{\Theta_{12}^4}{\left(4\Theta_{22}^2+2\left(\Delta w^{-2}+iD_m\Delta r\right)\right)}\right)^{-1/2} \\
&\times \exp\left(\frac{\Theta_2^4 - i2\Theta_2^2\left(t_2-S_m\Delta r\right) - \left(t_2-S_m\Delta r\right)^2}{4\Theta_{22}^2+2\left(\Delta w^{-2}+iD_m\Delta r\right)}\right) \exp\left(\frac{\left(\Theta_1^2+i\left(t_1-S_n\Delta r\right) - \dfrac{2i\Theta_{12}^2\left(t_2-S_m\Delta r\right)-2\Theta_2^2\Theta_{12}^2}{4\Theta_{22}^2+2\left(\Delta w^{-2}+iD_m\Delta r\right)}\right)^2}{4\Theta_{11}^2+2\left(\Delta w^{-2}-iD_n\Delta r\right) - \dfrac{\Theta_{12}^4}{\left(\Theta_{22}^2+\left(\Delta w^{-2}+iD_m\Delta r\right)/2\right)}}\right),
\end{aligned}
\tag{10}
$$

where

$$
\begin{aligned}
\Theta_{nm}^2 &= \sum_{e=1}^{E}\left(\Delta k_{en}^2 - 2\Delta k_{en}\Delta k_{em} + \Delta k_{em}^2\right) s_{g_e}^2 l_e r/2 & \Theta_2^2 &= \sum_{e=1}^{E}\left(\Delta k_{em}-\Delta k_{en}\right)\Delta S_{em} s_{g_e}^2 l_e r \\
\Theta_1^2 &= \sum_{e=1}^{E}\left(\Delta k_{en}-\Delta k_{em}\right)\Delta S_{en} s_{g_e}^2 l_e r & \Theta_{12}^2 &= \sum_{e=1}^{E}\Delta S_{en}\Delta S_{em} s_{g_e}^2 l_e r/2 \\
\Theta_{11}^2 &= \sum_{e=1}^{E}\Delta S_{en}^2 s_{g_e}^2 l_e r/2 & \Theta_{22}^2 &= \sum_{e=1}^{E}\Delta S_{em}^2 s_{g_e}^2 l_e r/2
\end{aligned}
\quad , \tag{11}
$$

Δz is the inter-element spacing of the TRM, and the probe source is at $\left[R_p, z_p\right]$.

Reverberation Uncertainty

An expression equivalent to Equation (10) has been obtained for boundary reverberation [4]. The reverberation intensity from a TRM may be written as

$$
\begin{aligned}
\left\langle p_{rev_{TRM}}(t_1,z_1)\,p_{rev_{TRM}}(t_2,z_2)\right\rangle &= \frac{8p^3}{\Delta z^2\, r^2(z_p)\, r^2(z_{rev})}\int_0^\infty dr_1\int_0^\infty dr_2 \sum_{n=1}^{N}\sum_{m=1}^{M}\frac{e^{i\left(k_{nm}r_1-k_n^* R_p-k_{n'm'}^* r_2+k_{n'}R_p\right)}}{R_p|k_n||k_{n'}|\sqrt{k_m k_{m'}}}\frac{\exp\left(-(r_1-r_2)^2/2l^2\right)}{l\sqrt{2p\, r_1 r_2}} \\
&\times\frac{\exp\left(-\Theta_{nn'mm'}^2\right) f_n(z_p)\, f_{n'}(z_p)\, f_n^- f_{n'}^- ss_{nm} ss_{n'm'} f_m^+ f_{m'}^+ f_m(z_1)\, f_{m'}(z_2)}{\sqrt{\left(\Theta_{22}^2+\left(\Delta w^{-2}+iD_{n'm'}r_2\right)/2\right)}\sqrt{\left(\Theta_{11}^2+\left(\Delta w^{-2}-iD_{nm}r_1\right)/2-\dfrac{\Theta_{12}^4}{\left(4\Theta_{22}^2+2\left(\Delta w^{-2}+iD_{n'm'}r_2\right)\right)}\right)}} \\
&\times\exp\left(\frac{\Theta_2^4-i2\Theta_2^2\left(t_2-S_{n'm'}r_2\right)-\left(t_2-S_{n'm'}r_2\right)^2}{4\Theta_{22}^2+2\left(\Delta w^{-2}+iD_{n'm'}r_2\right)}\right)\exp\left(\frac{\left(\Theta_1^2+i\left(t_1-S_{nm}r_1\right)-\dfrac{2i\Theta_{12}^2\left(t_2-S_{n'm'}r_2\right)-2\Theta_2^2\Theta_{12}^2}{4\Theta_{22}^2+2\left(\Delta w^{-2}+iD_{n'm'}r_2\right)}\right)^2}{4\Theta_{11}^2+2\left(\Delta w^{-2}-iD_{nm}r_1\right)-\dfrac{\Theta_{12}^4}{\left(\Theta_{22}^2+\left(\Delta w^{-2}+iD_{n'm'}r_2\right)/2\right)}}\right), \quad (12)
\end{aligned}
$$

where $k_{nm}=k_n+k_m$, $S_{nm}=S_n+S_m$, $D_{nm}=D_n+D_m$, l is the correlation length scale of the scatterers, f_n^- and f_m^+ are the downgoing and upgoing planewave decomposition of the m th mode, both obtained at the depth of the reverberating surface z_{rev}, and the angular dependence of scattering from the surface is described by the functions ss_{nm} and $ss_{n'm'}$. Note in Equation (12) that the definitions of the Θ_{ij} are taken from Equations (11) with Δk_n replaced with Δk_{nm}, Δk_m replaced with $\Delta k_{n'm'}$, etc. When the two integrals over range are evaluated an expression for the expected value of the reverberation intensity integrated over the ensemble of possible environments is obtained

$$
\begin{aligned}
\left\langle p_{rev_{TRM}}(t_1,z_1)\,p_{rev_{TRM}}(t_2,z_2)\right\rangle &= \frac{8p^4}{\Delta z^2\, r^2(z_p)\, r^2(z_{rev})R_p}\sum_{n=1}^{N}\sum_{m=1}^{M}\frac{e^{i\left(-k_n^* R_p+k_{n'}R_p\right)}\exp\left(-\Theta_{nn'mm'}^2\right)}{l\sqrt{t_1 t_2\dfrac{2p}{S_{nm}S_{n'm'}}}|k_n||k_{n'}|\sqrt{k_m k_{m'}}} \\
&\times f_n(z_p)\, f_{n'}(z_p)\, f_n^- f_{n'}^- ss_{nm} ss_{n'm'} f_m^+ f_{m'}^+ f_m(z_1)\, f_{m'}(z_2)\left(\Theta_{22}^2+\left(\Delta w^{-2}+i\left(\frac{D_{n'm'}}{S_{n'm'}}\hat{t}_2-D_{n'}R_p\right)\right)/2\right)^{-1/2} \\
&\times\left(\Theta_{11}^2+\left(\Delta w^{-2}-i\left(\frac{D_{nm}}{S_{nm}}\hat{t}_1-D_nR_p\right)\right)/2-\Theta_{12}^4\left(4\Theta_{22}^2+2\left(\Delta w^{-2}+i\left(\frac{D_{n'm'}}{S_{n'm'}}\hat{t}_2-D_{n'}R_p\right)\right)\right)^{-1}\right)^{-1/2} \quad ,(13) \\
&\times\left(\frac{1}{2l^2}+\left(\frac{1}{D_1}+\frac{C_4^2}{D_2}\right)S_{n'm'}^2\right)^{-1/2}\left(-2\frac{C_4}{D_2}S_{nm}S_{n'm'}+\left(\frac{1}{D_1}+\frac{C_4^2}{D_2}\right)S_{n'm'}^2+\frac{S_{nm}^2}{D_2}-\frac{G_2^2}{4A}\right)^{-1/2} \\
&\times\exp\left(\frac{BB^2}{4AA}-\frac{G_1^2}{4A}+\frac{C_1}{D_1}+\frac{C_3^2}{D_2}-\left(2i\frac{C_4C_3}{D_2}+i\frac{C_2}{D_1}\right)\hat{t}_2+2i\frac{C_3}{D_2}\hat{t}_1+2\frac{C_4}{D_2}\hat{t}_1\hat{t}_2-\left(\frac{1}{D_1}+\frac{C_4^2}{D_2}\right)\hat{t}_2^2-\frac{1}{D_2}\hat{t}_1^2\right)
\end{aligned}
$$

where $\hat{t}_1 = t_1 + S_n R_p - \min\left(S_n\right) R_p$ and $\hat{t}_2 = t_2 + S_{n'} R_p - \min\left(S_{n'}\right) R_p$ and where

$$
\begin{aligned}
&D_1 = 4\Theta_{22}^2 + 2/\Delta w^2 + 2i\hat{t}_2 D_{n'm'}/S_{n'm'} - 2iD_{n'}R_p \\
&C_3 = \Theta_1^2 + 2\Theta_2^2\Theta_{12}^2/D_1 \\
&C_4 = 2\Theta_{12}^2/D_1 \\
&D_2 = 4\Theta_{11}^2 + 2/\Delta w^2 - 2i\hat{t}_1 D_{nm}/S_{nm} + 2iD_n R_p - 4\Theta_{12}^4/D_1 \\
&G_1 = ik_{n'm'} - \left(2iC_3C_4/D_2 + 2i\Theta_2^2/D_1\right)S_{n'm'} + 2C_4 S_{n'm'}\hat{t}_1/D_2 - 2\left(1/D_1 + C_4^2/D_2\right)S_{n'm'}\hat{t}_2 \\
&G_2 = -2C_4 S_{nm} S_{n'm'} + 2\left(1/D_1 + C_4^2/D_2\right)S_{n'm'}^2 \\
&A = 1/2l^2 + \left(1/D_1 + C_4^2/D_2\right)S_{n'm'}^2 \\
&AA = -2C_4/D_2 S_{nm} S_{n'm'} + \left(1/D_1 + C_4^2/D_2\right)S_{n'm'}^2 + S_{nm}^2/D_2 - G_2^2/4A \\
&BB \square -i\left(k_{nm} - k_{n'm'}\right) - \left(2iC_3C_4/D_2 + 2i\Theta_2^2/D_1\right)S_{n'm'} + 2iC_3 S_{nm}/D_3 + 2C_4\left(S_{nm}\hat{t}_2 + S_{n'm'}\hat{t}_1\right) \\
&-2\left(1/D_1 + C_4^2/D_2\right)S_{n'm'}\hat{t}_2 - 2S_{nm}\hat{t}_1/D_2 - 2G_1G_2/4A
\end{aligned}
\quad . \tag{14}
$$

Scattering Uncertainty

The backscattering from an object ensonified by a TRM has a very similar form to Equation (13) with the exception that objects may scatter any of four ways in amplitude, yielding sixteen cross terms for the scattered intensity

$$
\begin{aligned}
&\left\langle p_{scat_{TRM}}\left(t_1, z_1\right) p_{scat_{TRM}}\left(t_2, z_2\right)\right\rangle = \frac{4p^2}{\Delta z^2 r^2\left(z_p\right) r^2\left(z_{scat}\right) R_{scat}^2 R_p} \sum_{n=1}^{N}\sum_{m=1}^{N}\sum_{n'=1}^{N}\sum_{m'=1}^{N} \frac{e^{i\left(\left(k_{nm} - k_{n'm'}^*\right)R_o - \left(k_n^* - k_{n'}\right)R_p\right)}}{\left|k_n\right|\left|k_{n'}\right|\sqrt{k_m k_{m'}}} \\
&\times \frac{f_n\left(z_s\right) f_{n'}\left(z_s\right) T_{nmn'm'} f_m\left(z_1\right) f_{m'}\left(z_2\right) \exp\left(-\Theta_{nmn'm'}^2\right)}{R_o\sqrt{\left(\Theta_{22}^2 + \left(\Delta w^{-2} + iD_{n'm'}R_o\right)/2\right)}\sqrt{\left(\Theta_{11}^2 + \left(\Delta w^{-2} - iD_{nm}R_o\right)/2 - \dfrac{\Theta_{12}^4}{\left(4\Theta_{22}^2 + 2\left(\Delta w^{-2} + iD_{n'm'}R_o\right)\right)}\right)}} \\
&\times \exp\left(\frac{\Theta_2^4 - i2\Theta_2^2\left(\hat{t}_2 - S_{n'm'}R_o\right) - \left(\hat{t}_2 - S_{n'm'}R_o\right)^2}{4\Theta_{22}^2 + 2\left(\Delta w^{-2} + iD_{n'm'}R_o\right)}\right) \exp\left(\frac{\left(\Theta_1^2 + i\left(\hat{t}_1 - S_{nm}R_o\right) - \dfrac{2i\Theta_{12}^2\left(\hat{t}_2 - S_{n'm'}R_o\right) - 2\Theta_2^2\Theta_{12}^2}{4\Theta_{22}^2 + 2\left(\Delta w^{-2} + iD_{n'm'}R_o\right)}\right)^2}{4\Theta_{11}^2 + 2\left(\Delta w^{-2} - iD_{nm}R_o\right) - \dfrac{\Theta_{12}^4}{\left(\Theta_{22}^2 + \left(\Delta w^{-2} + iD_{n'm'}R_o\right)/2\right)}}\right)
\end{aligned} \tag{15}
$$

where $\hat{t}_1 = t_1 + S_n R_p - \min\left(S_n\right) R_p$, $\hat{t}_2 = t_2 + S_{n'} R_p - \min\left(S_{n'}\right) R_p$ and

$$
T_{nmn'm'} = \left\{
\begin{matrix}
f_n^- f_{n'}^- ss_{nm}^{-+} ss_{n'm'}^{-+} f_m^+ f_{m'}^+ & + f_n^- f_{n'}^- ss_{nm}^{-+} ss_{n'm'}^{--} f_m^+ f_{m'}^- & + f_n^- f_{n'}^+ ss_{nm}^{-+} ss_{n'm'}^{+-} f_m^+ f_{m'}^- & + f_n^- f_{n'}^+ ss_{nm}^{-+} ss_{n'm'}^{++} f_m^+ f_{m'}^+ \\
+ f_n^- f_{n'}^- ss_{nm}^{--} ss_{n'm'}^{-+} f_m^- f_{m'}^+ & + f_n^- f_{n'}^- ss_{nm}^{--} ss_{n'm'}^{--} f_m^- f_{m'}^- & + f_n^- f_{n'}^+ ss_{nm}^{--} ss_{n'm'}^{+-} f_m^- f_{m'}^- & + f_n^- f_{n'}^+ ss_{nm}^{--} ss_{n'm'}^{++} f_m^- f_{m'}^+ \\
+ f_n^+ f_{n'}^- ss_{nm}^{+-} ss_{n'm'}^{-+} f_m^- f_{m'}^+ & + f_n^+ f_{n'}^- ss_{nm}^{+-} ss_{n'm'}^{--} f_m^- f_{m'}^- & + f_n^+ f_{n'}^+ ss_{nm}^{+-} ss_{n'm'}^{+-} f_m^- f_{m'}^- & + f_n^+ f_{n'}^+ ss_{nm}^{+-} ss_{n'm'}^{++} f_m^- f_{m'}^+ \\
+ f_n^+ f_{n'}^- ss_{nm}^{++} ss_{n'm'}^{-+} f_m^+ f_{m'}^+ & + f_n^+ f_{n'}^- ss_{nm}^{++} ss_{n'm'}^{--} f_m^+ f_{m'}^- & + f_n^+ f_{n'}^+ ss_{nm}^{++} ss_{n'm'}^{+-} f_m^+ f_{m'}^- & + f_n^+ f_{n'}^+ ss_{nm}^{++} ss_{n'm'}^{++} f_m^+ f_{m'}^+
\end{matrix}
\right\}. \tag{16}
$$

In Equation (17) the up and downgoing mode decompositions $f_n^{\pm}$ are evaluated at the depth of the scatterer z_{scat}. For a sphere, the scattering functions $s_{nm}^{\pm\pm}$ are given by Ingenito [6].

RESULTS

We show an example of the deterioration of TRM performance due to uncertainty in the sound speed profile. The environment is shown in the left panel of Fig. 1. A downward refracting sound speed profile in 140 m of water lies over a 5 m thick slow sediment layer with a density of 1 g/cm^3, a sound speed of 1,482 m/s and a bulk attenuation of 0.06 dB/λ. The basement has a sound speed of 1,562 m/s, a density of 1.8 g/cm^3 and a bulk attenuation of 0.1 dB/λ. An internal wave field generated by PROSIM [7,8] superimposes sound speed perturbations on the water column. A realization of these perturbations is shown in the right panel of Fig. 1. A full depth-spanning monostatic TRM sonar is deployed at the origin and ensonifies the waveguide at 2kHz with a 0 dB gain time reversed version of signals it receives from a 0 dB probe source deployed at a range of 10 km and a depth of 20 m. The TRM has a source spacing of 1 m. The TRM sonar receives reverberation from the sediment-water interface and scattering from a 10 m radius vacuum spherical target deployed at the probe source location. The sediment water interface has a correlation length scale of 8 cm (eliminating Bragg scattering effects) and a scattering strength conforming to Lambert's law

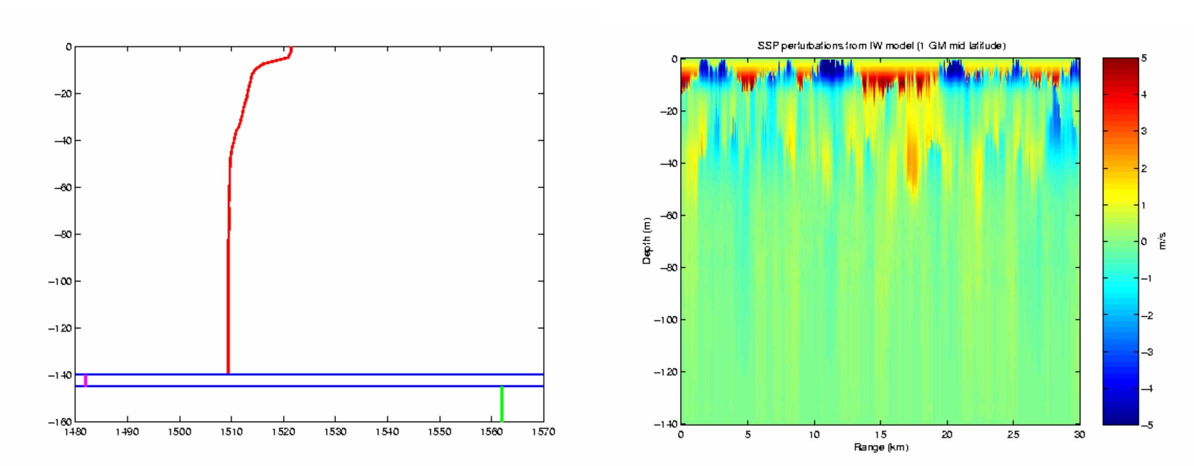

FIGURE 1. Sound speed profile of a typical shallow water environment (left). Superimposed sound speed perturbations caused by internal wave activity at the level of 1 GM (right).

$$SS_{nm} = -27 + 10\log 10\left\{ \sin\left[a\cos\left(k_n / k_o \right) \right] \sin\left[a\cos\left(k_m / k_o \right) \right] \right\}, \quad (17)$$

leading to the following expression for the surface scattering amplitude required in Equation 17

$$ss_{nm} = 10^{-27/20} \sqrt{\sin\left[a\cos\left(k_n / k_o \right) \right] \sin\left[a\cos\left(k_m / k_o \right) \right]}. \quad (18)$$

In the absence of the internal wave activity, the sphere is very strongly ensonified by the focused field at the probe source location, causing a strong echo. At the same time, the reverberation from the bottom is reduced in the vicinity of the target echo on the order of 40 dB. The presence of the strong focus makes possible the detection of the object by both increasing the incident pressure on the object and reducing the field incident on the scatterers beneath it [9][10].

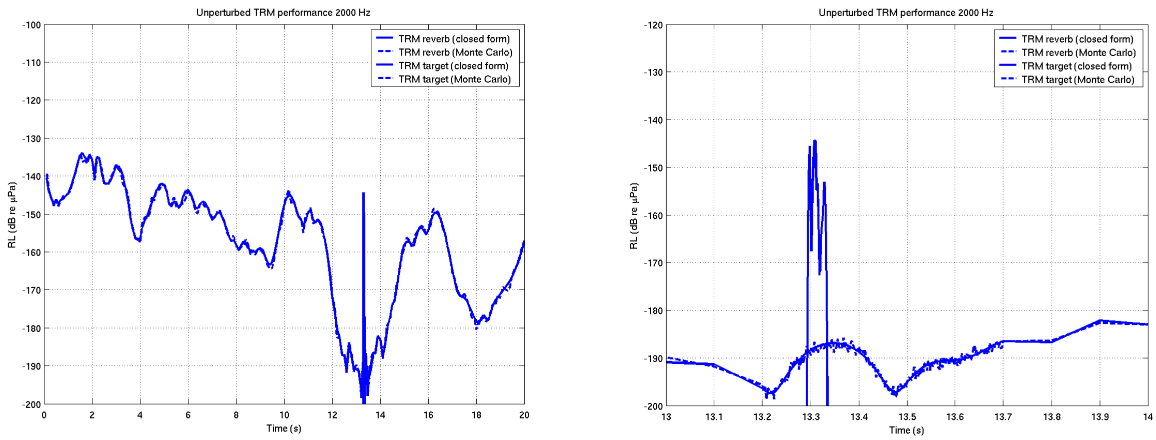

FIGURE 2. Reverberation and target echos in the environment of Figure 1 without internal wave activity. Left panel shows entire reverberation and echo time series, right panel is a close-up.

The uncertainty introduced by the presence of shallow water internal waves increases the expected value of the reverberation at the target range and reduces the expected value of the target echo, as shown in Figure 3.

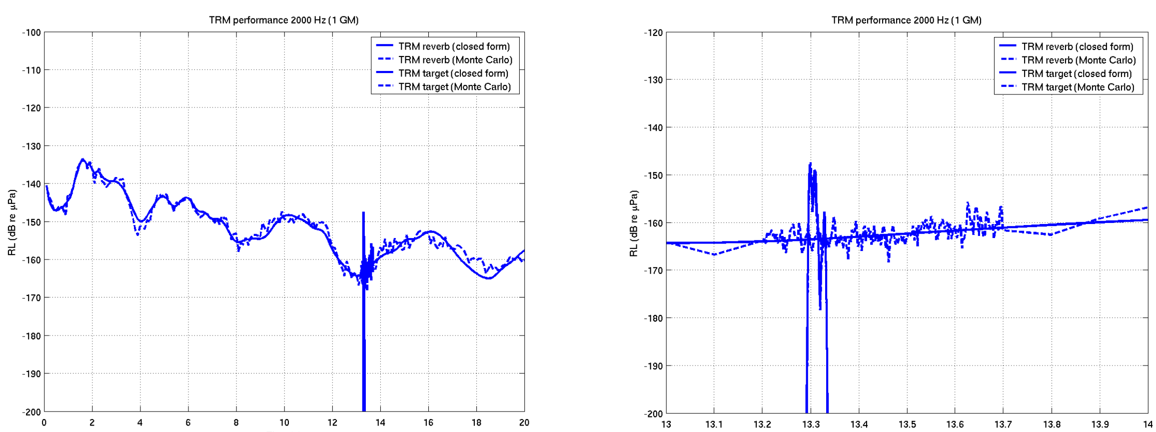

FIGURE 3. The expected value of bottom reverberation and target echo in the presence of internal waves. Left panel shows entire reverberation and echo time series, right panel is a close-up.

CONCLUSIONS

Expressions for the expected value of the second moment of acoustic pressure in the presence of environmental uncertainty have been obtained for propagation, reverberation and target echo caused by both point sources and TRMs. The expressions have been obtained for adiabatic propagation of normal modes through environmental variability. Results show that environmental uncertainty in the form of internal wave activity at the 1 GM level reduces the expected value of the coherent gain against bottom reverberation from 40 dB to 10 dB at 15 km for a 20 m probe source depth. The corresponding expected value of the backscattered intensity from a sphere at the probe source position is also reduced, by approximately 3 dB. The overall deterioration of SNR is, therefore, 33 dB. This prediction is believed to represent a lower bound on deterioration caused by environmental realizations. Inclusion of mode coupling effects and inhomogeneity of the environmental perturbations could be expected to seriously degrade the performance over and above the degradation predicted for adiabatic effects only.

ACKNOWLEDGMENTS

This work was funded under ONR's Capturing Uncertainty in the Common Tactical/Environmental Picture DRI.

REFERENCES

1. Krolik, J. L., *J. Acoust. Soc. Am.* **92**, 1408-1419 (1992).
2. LePage, K. D., *J. Comp. Acoust.* **9**, 1455-1474 (2001).
3. LePage, K. D., *Modeling Propagation and Reverberation Sensitivity to Oceanographic and Seabed Variability, SM-398*, La Spezia, Italy: SACLANT Undersea Research Centre, 2002.
4. Jensen, F.B., Kuperman, W.A., Porter, M.B., and Schmidt, H., *Computational Ocean Acoustics*, New York: AIP, 1993, pp. 274.
5. Sperry, B. J., McDonald, B.E., and Baggeroer, A.B., *J. Acoust. Soc. Am.* **114**, 1851-1860 (2003).
6. Ingenito, F., *J. Acoust. Soc. Am.* **82**, 2051-2059 (1987).
7. PROSIM (PROpagation channel SIMulator) First year technical report, TMS SAS 97/S/EGS/NC/084 AP (1998).
8. Elliot, A.J., and Jackson, J.F.E., "Internal Waves and Acoustic Variability," in *Proc. of the IEEE Oceans'98 Conference*, 1998, pp. 10-14.
9. Holland, C.W., and McDonald, B.E., *Shallow Water Reverberation from a Time Reversed Mirror, SR-326*, La Spezia, Italy: SACLANT Undersea Research Centre, 2000.
10. Lingevitch, J.F., Song, H.C., and Kuperman, W.A., *J. Acoust. Soc. Am.* **111**, 2609-2614 (2002).